Available online at www.sciencedirect.com
ScienceDirect
Electrochimica Acta 52 (2006) 1120–1126
ELECTROCHIMICA Acta
www.elsevier.com/locate/electacta

The influence of preparation conditions on electrochemical properties of $LiNi_{0.5}Mn_{1.5}O_4$ thin film electrodes by PLD

H. Xia [a], S.B. Tang [b], L. Lu [a,b,*], Y.S. Meng [c], G. Ceder [a,c]

[a] *Advanced Materials for Micro- and Nano-System, Singapore-MIT Alliance, 4 Engineering Drive 3, Singapore 117576, Singapore*
[b] *Department of Mechanical Engineering, National University of Singapore, 9 Engineering Drive 1, Singapore 117576, Singapore*
[c] *Department of Materials Science and Engineering, Massachusetts Institute of Technology, Cambridge, MA 02139, USA*

Received 18 May 2006; received in revised form 4 July 2006; accepted 11 July 2006
Available online 22 August 2006

Abstract

$LiNi_{0.5}Mn_{1.5}O_4$ thin films were prepared by pulsed laser deposition (PLD) on stainless steel substrates. The growth of the films has been studied as a function of substrate temperature and oxygen partial pressure in deposition, using X-ray diffraction (XRD) and field-emission scanning electron microscopy (FESEM). Electrochemical properties of $LiNi_{0.5}Mn_{1.5}O_4$ thin film cathodes were investigated using cyclic voltammetry and galvanostatic charge/discharge against a lithium anode. The initial capacity and capacity retention of the films are highly dependent on the crystallinity and purity of the films. $LiNi_{0.5}Mn_{1.5}O_4$ thin films grown at 600 °C in an oxygen partial pressure of 200 mTorr are well crystallized with high purity, exhibiting excellent capacity retention between 3 and 5 V with a $LiPF_6$-based electrolyte.
© 2006 Elsevier Ltd. All rights reserved.

Keywords: Thin-film battery; $LiNi_{0.5}Mn_{1.5}O_4$; Pulsed laser deposition

1. Introduction

Layered $LiCoO_2$, $LiNO_2$ and spinel $LiMn_2O_4$ are the most important cathode materials for Li-ion batteries because of their high operating voltage (4 V versus Li/Li^+) and good capacity retention. Among them, the spinel $LiMn_2O_4$ is the most favored one, especially for large sized batteries for electric vehicle (EV) applications, due to its lower cost and nontoxicity [1–3]. However, $LiMn_2O_4$ is not stable during cycling especially at elevated temperature, which results in a rapid capacity fade and hence limits its practical use [4–6]. Therefore, much research has been carried out to improve its charge and discharge cycle performance.

One excellent method for improving the cycle performance is the substitution of other transition metals for Mn to make $LiM_xMn_{2-x}O_4$ (M = Co [7], Cr [8], Ni [9], Fe [10], Cu [11], etc.). Interestingly, it has been found that this approach is also accompanied by a higher voltage plateau at about 5 V as a result of the redox system provided by the transition metal substituted. Materials of this group are now attractive candidates as cathode materials for lithium-ion batteries because they can increase the cell voltage to 5 V from the present 4 V. Within this group of materials, $LiNi_{0.5}Mn_{1.5}O_4$ is the most attractive material for the practical preparation of 5 V cathodes due to its high capacity and good stability on repeated Li-ion extraction and insertion [12–14].

Owing to the fact that the development in microelectronics industries has reduced the current and power requirements of electronic devices to an extremely low level, it is therefore possible the use of thin film batteries (TFBs) as power sources for these devices. Further more, thin film electrodes are ideal samples for studying the intrinsic properties of electrode materials because there are no binder and conductive additive in the films. Thin film electrodes have been successfully prepared by various techniques such as radio frequency (rf) sputtering [15], pulsed laser deposition [16], chemical vapor deposition [17], spin coating [18] and electrostatic spray deposition [19]. Among them, PLD is a powerful and easy method for producing high quality and dense films without post-deposition annealing. Studies on thin film electrodes have been mainly applied to $LiCoO_2$ and $LiMn_2O_4$. Very limited research [20,21] has been done on spinel $LiNi_{0.5}Mn_{1.5}O_4$ thin film electrodes.

In this work, we first report on the preparation and characterization of $LiNi_{0.5}Mn_{1.5}O_4$ thin films by PLD. Influences of

* Corresponding author. Fax: +65 6779 1459.
E-mail address: mpeluli@nus.edu.sg (L. Lu).

0013-4686/$ – see front matter © 2006 Elsevier Ltd. All rights reserved.
doi:10.1016/j.electacta.2006.07.013

both substrate temperature and oxygen partial pressure on the microstructure and morphology of $LiNi_{0.5}Mn_{1.5}O_4$ thin films are investigated. Electrochemical properties of $LiNi_{0.5}Mn_{1.5}O_4$ thin films are further characterized as a function of deposition conditions.

2. Experimental

Starting materials, MnO_2 99.9% (Alfa Aeser), NiO 99% (Alfa Aeser) and LiOH 98% (Merck) with appropriate molar ratios were mixed using ball mill for 2 h. The mixture was placed in an Al_2O_3 crucible and heated in air at 750 °C for 24 h. After grinding, the powder was cold-pressed into a pellet and subsequently fired in air at 900 °C for 2 h to densify the target. The $LiNi_{0.5}Mn_{1.5}O_4$ thin films were deposited on stainless steels (SS) and SiO_2/Si (SOS) substrates by PLD in a vacuum chamber at a base pressure less than 10^{-5} Torr. The target-substrate distance was kept at 35 mm. A Lambda Physik KrF excimer laser with wavelength 248 nm was used in the deposition. Laser fluence and repetition rate were respectively controlled at 2 J cm^{-2} and at 10 Hz. Film depositions were carried out at substrate temperatures ranging from 300 to 600 °C and in the oxygen partial pressures ranging from 50 to 200 mTorr for 40 min. All characterization and electrochemical measurements were performed on the films on SS substrates. Thin films on SOS substrates were only used for estimating the growth rate and thickness of the film. The amount of $LiNi_{0.5}Mn_{1.5}O_4$ was estimated by weighing the substrate before and after the film deposition using a microbalance (A&D, GR-202).

Structure and crystallinity of the thin films were measured using a Shimadzu XRD-6000 X-ray diffractometer with Cu Kα radiation. Data were collected in the range of 10–70° at a scan rate of 2°/min. Surface morphology and roughness of thin films were characterized using a Hitachi S-4100 field emission scanning electron microscopy (FESEM). The cross-sections of thin films on SOS substrates were observed by FESEM to estimate the thin film thickness and the growth rate. The thickness of thin films deposited at different conditions ranges from 300 to 500 nm.

Electrochemical experiments were conducted using a Solatron 1287 cell test system The electrochemical cell consisted of a Li-metal foil as the counter electrode, a $LiNi_{0.5}Mn_{1.5}O_4$ thin film of approximately 0.785 cm^2 of active area as the working electrode, and 1 M $LiPF_6$ in EC/DEC (1/1 vol.%) as the electrolyte. Galvanostatic charge/discharge measurements were carried out in the voltage range between 3 and 5 V with a current density of 20 μA/cm^2. Cyclic voltammogram (CV) measurements were carried out in the voltage range between 3.5 and 5 V with a scan rate of 0.2 mV/s.

3. Results and discussion

3.1. Structure characterization

The microstructure and crystallinity of $LiNi_{0.5}Mn_{1.5}O_4$ thin films are dependent on particular deposition conditions. One major factor is the substrate temperature, T_S. Fig. 1 shows the

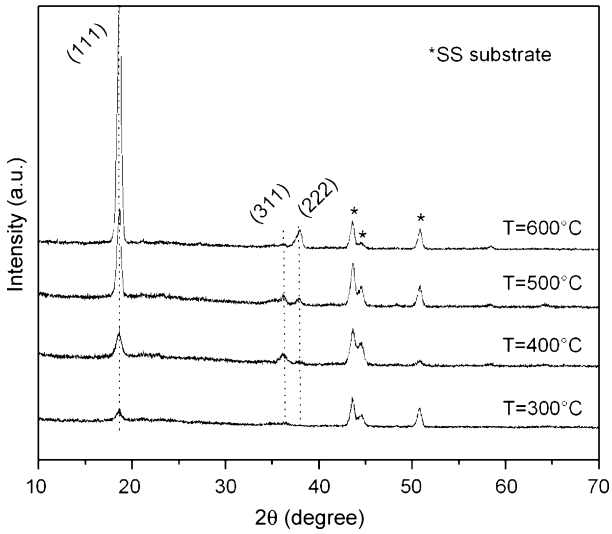

Fig. 1. XRD spectra of $LiNi_{0.5}Mn_{1.5}O_4$ thin films deposited at different substrate temperatures (T_S = 300, 400, 500 and 600 °C, P_{O_2} = 200 mTorr).

XRD spectra obtained from films deposited on SS substrates at different temperatures ranging from 300 to 600 °C with a constant oxygen partial pressure of 200 mTorr. All diffraction peaks attributed to the films can be indexed based on a spinel structure with space group $Fd\bar{3}m$. In this spinel-framework structure, the oxygen ions at the 32e sites form the cubic-close packing, in which Li atoms occupy the tetrahedral interstices (8a sites) and Ni and Mn atoms occupy the octahedral interstices (16d sites). One major peak from (1 1 1) diffraction is observed from all spectra and another two minor peaks of (3 1 1) and (2 2 2) are also observed from some spectra. When the film is deposited at the lowest substrate temperate of 300 °C in the present investigation, the XRD spectrum only shows a very weak diffraction peak of (1 1 1) indicating that the film is not well crystallized with an amorphous structure. With increase in the substrate temperature, the (1 1 1) peak increases rapidly and a (1 1 1) texture develops. This observation is similar to Chiu's study [22] on $LiMn_2O_4$ films by PLD. A sharp (1 1 1) peak is observed for the film deposited at 600 °C indicating good crystallinity.

Besides the effect of the substrate temperature, the oxygen partial pressure, P_{O_2}, during deposition is another important factor which can significantly affects the microstructure of $LiNi_{0.5}Mn_{1.5}O_4$ films. Fig. 2 shows the XRD spectra from films deposited on SS substrates at different oxygen partial pressures ranging from 50 to 300 mTorr at a constant substrate temperature of 600 °C. It is clear that all the films deposited at different oxygen partial pressures exhibit a (1 1 1) texture. The (1 1 1) texture increases with the increase in oxygen partial pressure. As the oxygen partial pressure increases (3 1 1) and (2 2 2) diffraction peaks became more obvious. At a very low oxygen partial pressure of 50 mTorr, diffraction peaks in this selected range are off from the peak positions of (3 1 1) and (2 2 2) indicating impurity phases exist in the film when deposited at very low oxygen partial pressure. From previous study [12] on $LiNi_{0.5}Mn_{1.5}O_4$ composite electrodes, the impurities such as NiO and $Li_xNi_{1-x}O$ were often observed in the final product after high temperature synthesis. From Rougier's study [23] on $LiMn_2O_4$ thin films

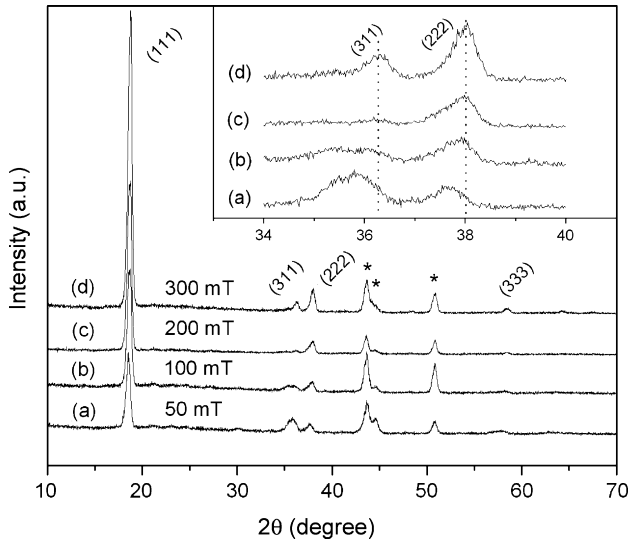

Fig. 2. XRD spectra of $LiNi_{0.5}Mn_{1.5}O_4$ thin films deposited at different oxygen partial pressures (T_S = 600 °C): (a) 50 mTorr, (b) 100 mTorr, (c) 200 mTorr and (d) 300 mTorr.

by PLD, Mn_2O_3 can be present as an impurity phase. Based on the positions of the impurity peaks for the film deposited at low oxygen pressure of 50 mTorr, it could be speculated the impurity phases existing in the film could be a combination of Mn_2O_3 and NiO. Such impurity peaks are not observed for the films deposited at high oxygen partial pressures like 200 and 300 mTorr.

3.2. Crystallinity and surface morphology

Fig. 3 shows the SEM images of the films deposited at different substrate temperatures. It can be seen that the substrate temperature played an important role on morphology evolution. At 300 °C, a lot of flake shaped particles are formed on the top of the film, which increases the surface roughness. The film underneath these discrete particles exhibits a nearly amorphous nature, without any obvious grains can be observed. At 400 °C, the amount of the discrete particles on the top of the film is reduced and the film is composed of small grains (<100 nm). At 500 °C, the flake shaped particles totally disappear, which creates a smooth surface, and the film is composed of bigger grains (~200 nm). At 600 °C, the film appears dense and smooth, and is composed of well-defined grains in the range between 200 and 300 nm. The grain shape reflects the spinel structure, a high proportion of octahedral or pseudo-polyhedral forms with well-defined edges and faces. When the substrate temperature is low, the adatom mobility is low and atoms are easy to cluster to form discrete particles, which results in a rough morphology. With the increase in deposition temperature, the particles are reduced and even removed due to the enhanced adatom mobility, which results in a smooth morphology.

Fig. 4 shows the SEM images of the films deposited at different oxygen partial pressures from 50 to 300 mTorr. All films deposited exhibit a smooth surface without big particles or droplets on the surfaces and are free of crack. At low oxygen partial pressure such as 50 and 100 mTorr, the films appear very dense but grains are not well defined. At high oxygen partial pressures of 200 and 300 mTorr, the grains are well defined but the density of pores in the film is increased. As the oxygen partial pressure increases, the average grain size also increases but not as obvious as the temperature effect. In general, raising the background pressure for PLD will result in attenuation and slowing of the plume. The deposition rate of the $LiNi_{0.5}Mn_{1.5}O_4$ film will be reduced when using a high oxygen pressure due to the enhanced collisional scattering. The reduced deposition rate will result in better crystallization.

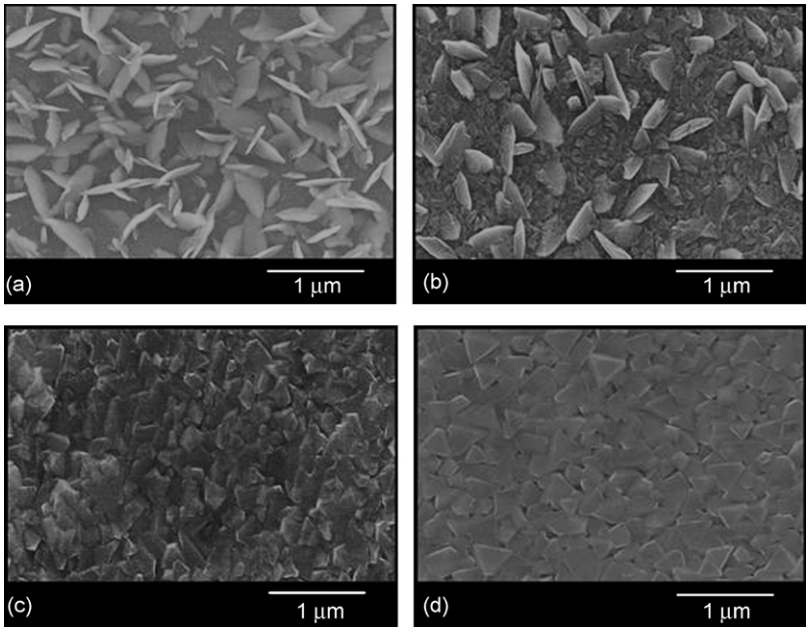

Fig. 3. SEM images of $LiNi_{0.5}Mn_{1.5}O_4$ thin films deposited at different substrate temperatures (P_{O_2} = 200 mTorr): (a) 300 °C, (b) 400 °C, (c) 500 °C and (d) 600 °C.

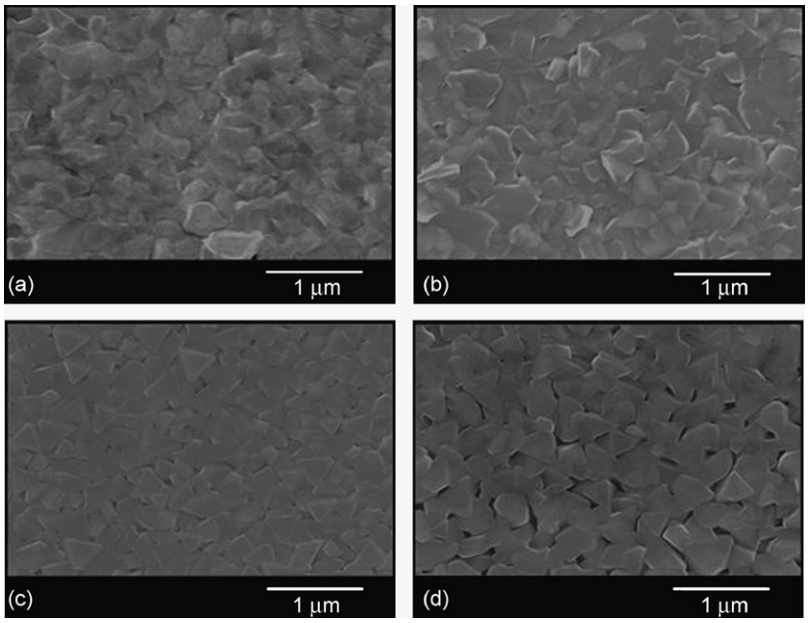

Fig. 4. SEM images of $LiNi_{0.5}Mn_{1.5}O_4$ thin films deposited at different oxygen partial pressures ($T_S = 600\,^{\circ}C$): (a) 50 mTorr, (b) 100 mTorr, (c) 200 mTorr and (d) 300 mTorr.

3.3. Electrochemical characterization

Fig. 5 shows a typical CV of the $LiNi_{0.5}Mn_{1.5}O_4$ film deposited at $T_S = 600\,^{\circ}C$, $P_{O_2} = 200$ mTorr in the voltage range from 3.5 to 5 V with a scan rate of 0.2 mV/s. As shown in Fig. 5, three pairs of reversible peaks can be observed with two pairs of major peaks (A2–C2 and A3–C3) at high voltages about 4.7 V and one pair of minor peaks (A1–C1) at about 4 V. For the $LiMn_2O_4$ electrode, Li-ion intercalation/deintercalation take place with the redox of $Mn^{3+/4+}$ at about 4 V. In case of $LiNi_{0.5}Mn_{1.5}O_4$, substitution metal ions (Ni^{2+}) exist at 16d sites instead of Mn^{3+} and all Mn ions should exist in 4+ oxidation state. The high voltage peaks at 4.68 (A1) and 4.79 V (A2) on anodic scan, and at 4.65 (C1) and 4.75 V (C2) on cathodic scan should correspond to the redox reactions of Ni^{2+}/Ni^{3+} and

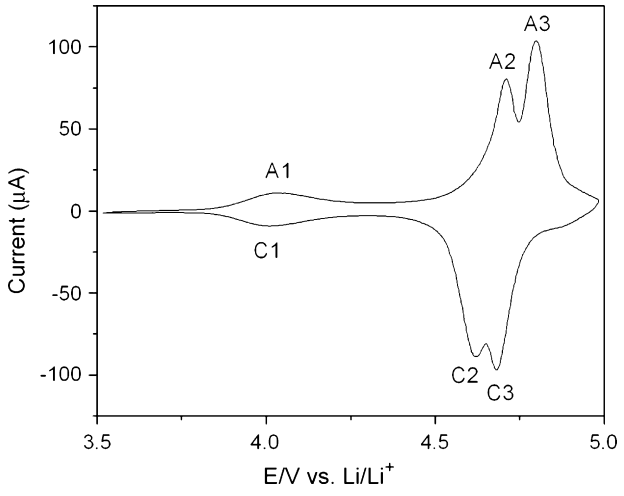

Fig. 5. Typical cyclic voltammogram of the $LiNi_{0.5}Mn_{1.5}O_4$ thin film electrode prepared at $T_S = 600\,^{\circ}C$ and $P_{O_2} = 200$ mTorr.

Ni^{3+}/Ni^{4+}. Dahn et al. [24] suggested that the electrode potential of $LiMn_2O_4$ could be enhanced from 4 to 4.7 V by a substitution of a part of Mn ions in $LiMn_2O_4$. They have discussed the appearance of the 4.7 V electrode potential regions by using UV photoelectron spectroscopy and have claimed that energy of 3d level for Ni^{2+} ion and Ni^{3+} ion in a low spin state is lower than that of Mn^{3+} ion in a high spin state. Such a difference between energies for 3d levels leads to a higher electrode potential of $LiNi_{0.5}Mn_{1.5}O_4$. The tiny peaks at 4 V in Fig. 5 should correspond to the redox reaction of $Mn^{3+/4+}$, which indicates existence of a small amount of Mn^{3+} ions in the film. For a pure phase spinel $LiNi_{0.5}Mn_{1.5}O_4$ film, this 4 V signal should not be observed from the CV. The existence of Mn^{3+} ions in the spinel $LiNi_{0.5}Mn_{1.5}O_4$ was often observed from previous studies on composite electrodes [12,25,26]. There are probably two mechanisms to explain the formation of Mn^{3+} ions. The first is nickel deficiency. The nickel deficiency stems from the formation of secondary phases of NiO or $Li_xNi_{1-x}O$ in the calcined powders [12], which leads to less nickel in the spinel phase. The second is oxygen deficiency. The oxygen deficiency [12,26] is due to the oxygen loss at high calcination temperature. Once the oxygen deficiency takes place, the average valence of manganese would decrease owing to the charge balance compensation, causing reduction of some small portion of Mn from 4+ to 3+. In present investigation, the thin film was deposited in a vacuum state with a high substrate temperature ($T_S = 600\,^{\circ}C$), which probably induced some oxygen loss and Ni-based impurities resulting in a small amount of Mn^{3+} ions in the film.

Electrochemical properties of $LiNi_{0.5}Mn_{1.5}O_4$ thin films are highly dependent on the microstructure and morphology of the films. Typical charge/discharge curves of $LiNi_{0.5}Mn_{1.5}O_4$ thin films deposited at different substrate temperatures but at the same oxygen partial pressure 200 mTorr are shown in Fig. 6. The specific capacity was calculated based on the thin film weight

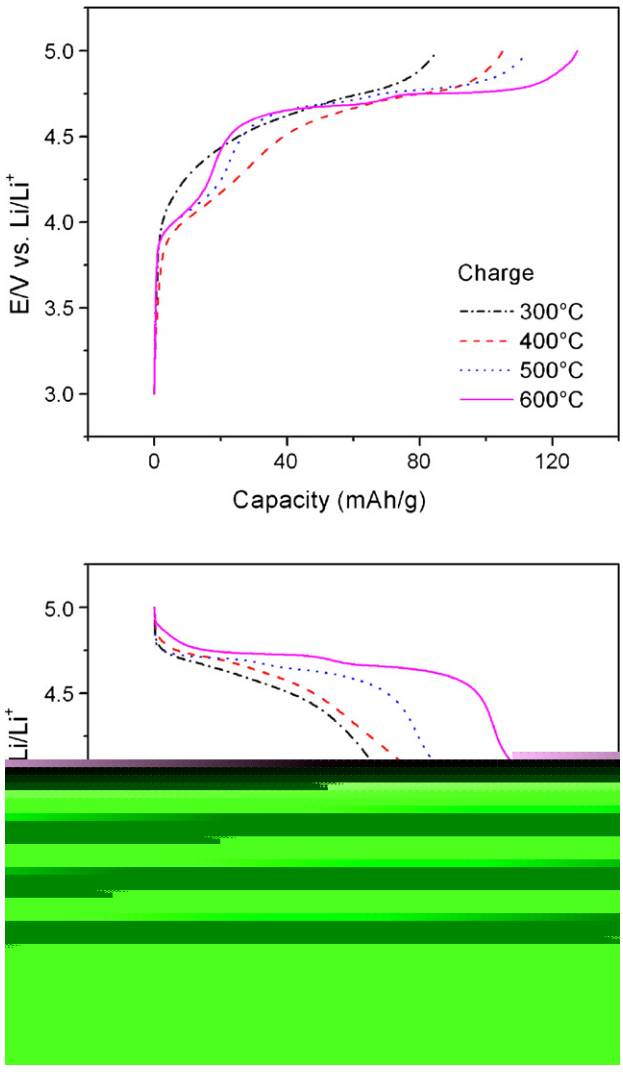

Fig. 6. Typical charge/discharge curves of $LiNi_{0.5}Mn_{1.5}O_4$ thin films deposited at different substrate temperatures (P_{O_2} = 200 mTorr): T_S = 300, 400, 500 and 600 °C.

(about 0.2–0.3 mg/cm^2) measured by the microbalance. At very low substrate temperature of 300 °C, the charge/discharge curves of the film exhibit slope profiles between 4 and 5 V without any voltage plateau caused by poor crystallization of thin film. This observation agrees with the XRD and SEM results. As the substrate temperature increases, three voltage plateaus develop for both charge and discharge. At the substrate temperature of 600 °C, both charge and discharge curves show three well-defined voltage plateaus at 4, 4.6 and 4.7 V, respectively. The charge/discharge curves of the well-crystallized $LiNi_{0.5}Mn_{1.5}O_4$ film agree well with the CV result, where the peaks in CV correspond to the voltage plateaus in charge/discharge. As shown in Fig. 6, the reversible capacities of the films deposited at 300, 400, 500 and 600 °C are 82.1, 100.3, 106.7 and 122.5 mAh/g, respectively. The theoretical capacity of pure spinel $LiNi_{0.5}Mn_{1.5}O_4$ is 146.6 mAh/g. It is clear to see a development of the capacity as a function of the substrate temperature. As the substrate temperature increases, the reversible capacity and utilization of the film increases. The difference between the voltage plateaus for charge and discharge indicates the polarization of the cell, which is caused by the cell resistance. As shown in Fig. 6, the film deposited at 600 °C exhibit the smallest polarization compared with rest samples. This result suggested that the diffusion and migration of Li ions are faster in the film deposited at 600 °C than those in other films deposited at lower temperatures, which probably explains the highest reversible capacity and utilization of the film. Therefore, the substrate temperature is crucial for obtaining electrochemically active $LiNi_{0.5}Mn_{1.5}O_4$ with a well-crystallized spinel structure.

Typical charge/discharge curves of $LiNi_{0.5}Mn_{1.5}O_4$ thin films deposited at different oxygen partial pressures but at the same substrate temperature 600 °C are shown in Fig. 7. Though the substrate temperature is high, the charge/discharge curves of the film deposited at low oxygen partial pressure of 50 mTorr exhibit sloppy voltage plateaus, which indicates the film may not be well-crystallized. Similar to the substrate temperature effect, well-defined voltage plateaus develop as the oxygen partial pressure increases. Though high oxygen partial pressure may also improve the crystallinity of the film, the effect of oxygen

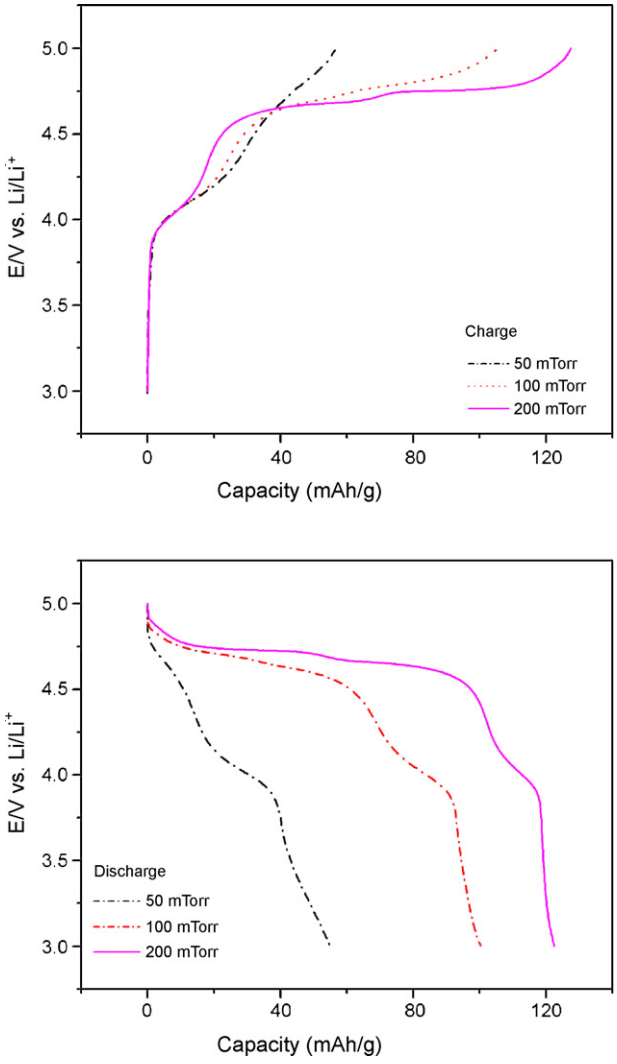

Fig. 7. Typical charge/discharge curves of $LiNi_{0.5}Mn_{1.5}O_4$ thin films deposited at different oxygen partial pressures (T_S = 600 °C): P_{O_2} = 50, 100 and 200 mTorr.

film electrodes fabricated by Mohamedi et al. [20]. Both thin film electrodes show high capacity and good capacity retention. However, the ESD thin film electrode shows higher reversible capacity (over 140 mAh/g) than that of the present film (about 120 mAh/g). Comparing CV curves for both thin film electrodes, we found that the ESD film exhibit almost no 4 V peak which means there is almost no Mn^{3+} ion existing in their film. For the PLD, since the film is deposited in vacuum state, it is clear shown that there exists an oxygen deficiency at low oxygen partial pressure leading to the presence of a small amount of Mn^{3+} ions. Therefore, it can be speculated that high purity of the ESD film offers the higher capacity. Though the PLD film exhibits relatively lower capacity, it shows higher capacity retention than the ESD film. The retaining capacities of each initial capacity after 50 cycles are 91% and 96% for the ESD and PLD film, respectively. We attribute the better capacity retention of the PLD film to the in situ heating of the PLD system which uses lower annealing temperature (600 °C for PLD, 700 °C for ESD). The lower crystallization temperature and simple heating process probably result in a denser film without crack (which is confirmed by the SEM), which is supposed to reduce the loss of active material during Li intercalation/deintercalation process and results in better capacity retention.

In addition to capacity retention, kinetics of Li-ion intercalation/deintercalation into the $LiNi_{0.5}Mn_{1.5}O_4$ film which determines the rate capability of this material is another important property to study. From previous work obtained by Mohamedi et al. [20], the chemical diffusion coefficient of Li in the ESD $LiNi_{0.5}Mn_{1.5}O_4$ film varies from 10^{-12} to 10^{-10} cm^2/s. High rate capability is expected from this material due to this high Li diffusivity.

4. Conclusions

Spinel $LiNi_{0.5}Mn_{1.5}O_4$ thin films were successfully prepared on the SS substrates by PLD. The microstructure and surface morphology of thin films are highly affected by the substrate temperature and oxygen partial pressure. A high degree of crystallinity and smooth surface morphology can only be achieved at high substrate temperatures. Impurity formed during deposition and a small amount of Mn^{3+} ions in the film can be reduced by increasing the oxygen partial pressure. Thin films with better crystallization and less impurity exhibit better electrochemical properties. Thin films deposited at $T_S = 600\,^{\circ}C$ and $P_{O_2} = 200$ mTorr has the highest electrochemical activity, showing the largest initial capacity, best capacity retention and only a very small 4 V plateau. Well-crystallized $LiNi_{0.5}Mn_{1.5}O_4$ thin films show very stable cycle performance between 3 and 5 V, which are promising thin film cathodes for fabricating 5 V microbatteries.

Acknowledgements

This research was supported by Advanced Materials for Micro- and Nano-System (AMM&NS) programme under Singapore-MIT Alliance (SMA) and by National University of Singapore.

References

[1] T. Ohzuku, M. Kitagawa, T. Hirai, J. Electrochem. Soc. 137 (1990) 769.
[2] J.M. Tarascon, E. Wang, F.K. Shokoohi, W.R. Mckinnon, S. Colson, J. Electrochem. Soc. 138 (1991) 2859.
[3] J.M. Tarascon, D. Guyomard, Electrochim. Acta 38 (1993) 1221.
[4] R.J. Gummow, A. de Kock, M.M. Thackeray, Solid State Ionics 69 (1994) 59.
[5] S.J. Wen, T.J. Richardson, L. Ma, K.A. Striebel, P.N. Ross Jr., E.J. Cairns, J. Electrochem. Soc. 143 (1996) L136.
[6] Y. Xia, Y. Zhou, M. Yoshio, J. Electrochem. Soc. 144 (1997) 2593.
[7] H. Kawai, M. Nagata, H. Kageyama, H. Tukamoto, A.R. West, Electrochim. Acta 45 (1999) 315.
[8] C. Sigala, D. Guyomard, A. Verbaere, Y. Piffard, M. Tournoux, Solid State Ionics 81 (1995) 167.
[9] K. Amine, H. Tukamoto, H. Yasuda, Y. Fujita, J. Power Source 68 (1997) 604.
[10] H. Shigemura, H. Sakaebe, H. Kageyama, H. Kobayashi, A.R. West, R. Kanno, S. Morimoto, S. Nasu, M. Tabuchi, J. Electrochem. Soc. 148 (2001) A730.
[11] Y.E. Eli, W.F. Howard Jr., S.H. Lu, S. Mukerjee, J. Mcbreen, J.T. Vaughey, M.M. Thackeray, J. Electrochem. Soc. 145 (1998) 1238.
[12] Q. Zhong, A. Bonakdarpour, M. Zhang, Y. Gao, J.R. Dahn, J. Electrochem. Soc. 144 (1997) 205.
[13] T. Ohzuku, S. Takeda, M. Iwanaga, J. Power Sources 81 (1999) 90.
[14] M. Yoshio, T. Konishi, Y.M. Todorov, H. Noguchi, Electrochemistry 68 (2000) 412.
[15] N.J. Dudney, J.B. Bates, R.A. Zuhr, S. Young, J.D. Robertson, H.P. Jun, S.A. Hackney, J. Electrochem. Soc. 146 (1999) 2455.
[16] Y. Iriyama, M. Inaba, T. Abe, Z. Ogumi, J. Power Sources 94 (2001) 175.
[17] W.G. Choi, S.G. Yoon, J. Power Sources 125 (2004) 236.
[18] J.P. Maranchi, A.F. Hepp, P.N. Kumta, Mater. Sci. Eng. B 116 (2005) 327.
[19] M. Mohamedi, D. Takahashi, T. Itoh, M. Umeda, I. Uchida, J. Electrochem. Soc. 149 (2002) A19.
[20] M. Mohamedi, M. Makino, K. Dokko, T. Itoh, I. Uchida, Electrochim. Acta 48 (2002) 79.
[21] A. Caballero, L. Hernan, M. Melero, J. Morales, R. Moreno, B. Ferrari, J. Power Sources, in press.
[22] K.F. Chiu, H.H. Hsiao, G.S. Chen, H.L. Liu, J.L. Her, H.C. Lin, J. Electrochem. Soc. 151 (2004) A452.
[23] A. Rougier, K.A. Striebel, S.J. Wen, E.J. Cairns, J. Electrochem. Soc. 145 (1998) 2975.
[24] Y. Gao, K. Myrtlc, M. Zhang, J.N. Rcimers, J.R. Dahn, J. Electrochem. Soc. 144 (1997) 205.
[25] K. Kanamura, W. Hoshikawa, T. Umegaki, J. Electrochem. Soc. 149 (2002) A339.
[26] S.T. Myung, S. Komaba, N. Kumagai, H. Yashiro, H.T. Chung, T.H. Cho, Electrochim. Acta 47 (2002) 2543.
[27] J.H. Kim, S.T. Myung, Y.K. Sun, Electrochim. Acta 49 (2004) 219.
[28] G.Q. Liu, Y.J. Wang, W. Qilu, L. Chenhui, Electrochim. Acta 50 (2005) 1965.
[29] D. Kovacheva, B. Markovsky, G. Salitra, Y. Talyosef, M. Gorova, E. Levi, M. Riboch, H.J. Kim, D. Aurbach, Electrochim. Acta 50 (2005) 5553.
[30] K. Dokko, N. Anzue, M. Mohamedi, T. Itoh, I. Uchida, Electrochem. Commun. 6 (2004) 384.
[31] K. Dokko, N. Anzue, Y. Makino, M. Mohamedi, T. Itoh, M. Umeda, I. Uchida, Electrochemistry 71 (2003) 1061.